

1

2

3 Identification of mercury species in minerals with different  
4 matrices and impurities by thermal desorption technique

5

6

7 David Melero, Belén Lobato, Maria Antonia López-Antón\*, Maria Rosa Martínez-  
8 Tarazona

9

10

11 <sup>a</sup>Instituto Nacional del Carbón (CSIC), Francisco Pintado Fe, 26, 33011, Oviedo, Spain

12

13

14 \*Corresponding author:

15 Phone: +34 985 119090

16 Fax: +34 985 297662

17 Email: [marian@incar.csic.es](mailto:marian@incar.csic.es)

1 **Abstract**

2 Because of its low concentration, its unique physico-chemical properties and the  
3 analytical difficulties associated with its measurement, the determination of mercury  
4 species in solids is not an easy task. Thermal desorption (HgTPD) is an attractive option  
5 for the identification of mercury species in solids due to its simplicity and accessibility.  
6 However, there are still issues that need to be solved for it to reach its full potential. One  
7 such issue is the availability of reference materials that will reproduce real mercury  
8 associations. The novelty of this study is the use of six uncommon mercury minerals,  
9 taken from around the world, and a sphalerite sample to expand the data base of  
10 reference materials for mercury speciation by thermal desorption at programmed  
11 temperature. In addition, by using such materials, a number of matrix effects can be  
12 ascertained. Different mercury associations were identified depending on the  
13 temperature of desorption, thereby validating the thermal desorption as a reliable  
14 technique for mercury speciation in solid samples and as a consequence improving the  
15 knowledge of the geochemistry of mercury in the environment.

16

17

18 **Keywords:** mercury; minerals; thermal desorption; speciation; geochemistry

19

## 1. Introduction

Mercury is a metal that is well-known for its high toxicity and detrimental effects on health and the environment (WHO 2017). This unquestionable concern makes the identification of mercury species in solids critical for understanding and monitoring mercury-contaminated materials and soils. The Global Mercury Cycle is one of the most interesting and scientifically challenging biogeochemical cycles at the Earth's surface. A particular mercury speciation determines its bioavailability, environmental mobility and toxicity. Moreover the mode of occurrence of mercury also determines the choice of a suitable remediation method for its control (Rallo et al. 2012).

A variety of techniques have already been studied to identify mercury species in solids. The most consistent are: (i) sequential selective extractions (SSEs) (Biester and Scholz 1996; Bloom et al. 2003; Han et al. 2003; Issaro et al. 2009), (ii) extended X-ray absorption fine structure spectroscopy (EXAFS) (Huggins et al. 2003; Kim et al. 2003; 2004[6-8] and (iii) thermal programmed desorption (HgTPD) (Biester et al. 2002; Raposo et al. 2003, Reis et al. 2012; Rumayor et al. 2013; 2016). Each one of these techniques has inherent methodological limitations. SSEs is lacking in selectivity, EXAFS has high limits of detection ( $1 \text{ mg kg}^{-1}$ ), and in HgTPD matrix effects may be missed due to the common use of pure mercury compounds as reference materials. HgTPD is an easily accessible technique that can be implemented with simple instrumentation and requires less time for sample pre-treatment than EXAFS and SSE. However, the validity of the HgTPD method must remain open to doubt until the influence of several parameters upon the results can be clearly established. Among these parameters, matrix effects are a clear priority.

1        Although the dilemma about the best method for mercury speciation has not been  
2 solved, in the present study the method of HgTPD has been chosen and refined. Up until  
3 now the identification of mercury species in solids by HgTPD relied on the comparison  
4 of a sample desorption profile with the desorption profiles of commercial pure  
5 compounds (Lopez-Anton et al. 2010; Rumayor et al. 2013). However, the selection and  
6 preparation of other mercury reference materials is a key issue that needs to be  
7 addressed to account for potential matrix effects and to confirm the reliability of the  
8 technique. There is a need to determine whether the thermograms obtained with  
9 mercury pure compounds correspond with those obtained from real samples where the  
10 mercury species are associated to complex matrices. In addition, it is necessary to  
11 identify mercury species in common and rare mineral phases, such as sphalerite,  
12 edgarbaileyite, myrickite, and others, that are present in nature. Once each mercury  
13 species is matched to a characteristic desorption temperature, the HgTPD method will  
14 allow the identification of mercury species in contaminated and natural associations,  
15 which is the final goal pursued with this study.

16        Although mercury is mostly found in nature in the form of cinnabar (red HgS), and  
17 this is the primary mercury species to be used as a mercury reference, mercury can also  
18 be found in a wide range of complex minerals and complementary polymetallic ores  
19 such as livingstonite ( $\text{HgSb}_4\text{S}_8$ ), corderoite ( $\text{Hg}_3\text{S}_2(\text{Cl},\text{Br})_2$ ), edgarbaileyite ( $\text{Hg}_6\text{Si}_2\text{O}_7$ ),  
20 etc. (Kozin et al. 2015). Some of these minerals can be found in areas close to mercury  
21 mining and processing activities which are sources of pollution regarded as of primary  
22 environmental concern (Jiménez-Moreno et al. 2016; Kobal et al. 2017; Matanzas et al.  
23 2017; Yin et al. 2017). The analysis of the minerals containing mercury by HgTPD may  
24 be a useful tool for identifying sources of pollution related to mercury-mining or

1 metallurgy and for distinguishing them from other sources such as coal combustion or  
2 chlor-alkali industry.

3 These minerals are difficult replicate from the pure species that constitute the  
4 mercury reference materials. For example, edgarbaileyite is the first reported structure  
5 to contain both Hg and Si (Angel et al. 1990). It is also difficult to prepare standards  
6 that simulate other mercury sources in nature such as sphalerite, where mercury is often  
7 present as an impurity usually related to Zn smelters. Intrusive magmatic rocks and  
8 subaerial and submarine volcanic regions may contain high mercury concentrations. In  
9 these rocks values may be as high as several percent in ore-grade minerals (e.g., 35%  
10 mercury in sphalerite) (Ozerova 1996). Mercury desorption in these types of minerals  
11 and rocks has barely been studied although potentially they represent significant natural  
12 standards required for applying the HgTPD technique on the basis of their characteristic  
13 mercury desorption temperatures. To fill this gap, in this study a series of mercury  
14 minerals and rocks are evaluated by thermal desorption, improving the current database  
15 on the basis of which mercury species can be identified from their desorption  
16 temperature.

17

## 18 **2. Experimental part**

### 19 2.1 Mineral samples

20 Six mercury-containing mineral samples (coloradoite (Mine Bessie G, La Plata,  
21 Colorado, USA), edgarbaileyite (Clear Creek, S. Benito, California, USA), myrickite  
22 (Myrick Spring, Napa, California, USA), livingstonite (Guadalcazar, Potosí, Mexico),  
23 terlinguaite (Emerald Lake District, San Mateo Country, California, USA) and  
24 corderoite (Mine Usagre, Badajoz, Spain) and a sphalerite mineral (Mine Troya,  
25 Mutiloa, Guipuzkoa, Spain) were chosen for assessing the potential of HgTPD analysis

1 (Figure 1). The samples constitute a broad spectrum, including a natural mercury  
2 silicate (1 sample), natural mercury sulphides (4 samples), a natural mercury telluride (1  
3 sample), and a natural mercury oxychloride (1 sample).

4 The grinding and homogenization of mineral samples for their analysis was carried  
5 out by crushing the sample in a mortar to a particle size  $< 0.1$  mm. The composition of  
6 the mineral and its impurities was identified by Scanning Electron Microscopy (SEM)  
7 equipped with Energy Dispersive Analytical Systems (EDAS). The analysis was  
8 performed in the samples before and after grinding.

## 9 2.2 Hg-thermo-desorption device

10 The HgTPD device consists of a temperature-programmed furnace coupled to a  
11 PYRO 915 furnace from LUMEX and a continuous mercury analyzer (RA-915)  
12 (Rumayor et al 2015a). The peculiarity of this device, developed by the authors  
13 (Rumayor et al 2015b), is that the mercury species are desorbed in the first furnace  
14 using  $N_2$  as an inert gas, while at the same time  $O_2$  is introduced into the PYRO furnace  
15 to ensure the total decomposition of volatile matter. The solid is weighed in a sample  
16 boat where temperature is controlled by a thermocouple. Desorption profiles are  
17 obtained by heating the sample at a rate of  $50\text{ }^\circ\text{C min}^{-1}$  under a  $N_2$  flow of  $500\text{ mL min}^{-1}$ .  
18 The PYRO 915 unit is kept approximately at  $800^\circ\text{C}$  under an  $O_2$  flow of  $500\text{ mL min}^{-1}$ .  
19 In this unit all mercury species, vaporized from the sample in the inert atmosphere,  
20 are transformed into elemental gaseous mercury ( $Hg^0$ ).

21 As  $Hg^0$  reaches the detector in the continuous analyzer, the software registers  
22 temperature or time versus mercury and records the desorption profiles that correspond  
23 to evaporation of the mercury species present in the sample. As already described, each  
24 desorption peak is assigned to each species of mercury by using the reference data base

1 of different pure mercury compounds. The pure compounds used in this work as  
2 reference were Hg<sup>0</sup> and HgS, as they are the most likely species to be present in  
3 mercury minerals, and HgO and HgCl<sub>2</sub>, which are also possible. All samples were  
4 analyzed sequentially with the reference pure compound.

5 Overlapping peaks were deconvoluted using Origin 6.0 software.

6

### 7 **3. Results and discussion**

8 The thermograms of the mercury pure compounds and mineral samples containing  
9 mercury are shown in Fig. 2. Table 1 shows the maximum temperature of  
10 decomposition (high peak temperature) of each pure mercury compound registered in  
11 Fig. 2A. The precision of the analysis has been established from the results of the  
12 standard deviation obtained after analyzing each sample in triplicate.

13 Fig. 2B shows the thermal desorption profile of sphalerite. Sphalerite ((Zn, Fe) S) is  
14 not a mercury mineral, it is a zinc sulfide mineral in crystalline form with variable  
15 amounts of iron (0.3-2.5 wt%) (Grammatikopoulos et al. 2006), usually found in  
16 association with dolomite (CaMg(CO<sub>3</sub>)<sub>2</sub>) and siderite (FeCO<sub>3</sub>) (Fig. 1A, Fig. 3).  
17 However, this mineral may also contain variable amounts of mercury (0.1-16% wt%)  
18 (Grammatikopoulos et al. 2006). Sphalerite is usually associated with cinnabar and  
19 several sulfides, sulphosalts and non-opaque minerals. The thermogram of mercury  
20 species from the sphalerite sample analyzed showed a broad peak between 400-1000°C  
21 (Fig. 2B). This wide band does not correspond to the signal of any of the pure mercury  
22 compounds studied so far, suggesting that mercury with Zn and Fe sulfide may form  
23 stronger associations that result in these high desorption temperatures. Mercury in  
24 sphalerite could be also found as HgS impurity. In fact, the thermogram of this mineral  
25 showed a small peak around 200°C that can be assigned to HgS (Fig. 2B).

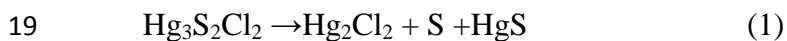
1 Coloradoite is the name of the mercury telluride (HgTe) mineral (Fig. 1C). It is a  
2 telluride ore associated with metallic deposits (especially gold and silver) (Fadda et al.  
3 2005). It is a mineral that belongs to group 16 of the chalcogen family of elements,  
4 which includes HgS. Even though the type of thermal desorption could be expect to be  
5 slightly different than that of HgS, by similarity to was observed to occur with the  
6 halide family (Lopez-Anton et al. 2010; Rumayor et al. 2013), the analysis by HgTPD  
7 showed that the maximum desorption peak of coloradoite overlaps with that obtained  
8 for HgS (Fig. 2C). It should be noticed that the analysis by SEM/EDAS (Fig. 4) of the  
9 mineral individual particles before and after grinding confirms that the only mercury  
10 species in the sample studied was HgTe.

11 Myrickite is the name for both agatized and opalized cinnabar (HgS SiO<sub>2</sub>) (Fig. 1B)  
12 It is only found overlying gold deposits. Analysis by SEM/EDAS of the sample  
13 corroborated the HgS/SiO<sub>2</sub> association (Fig. 5a). The presence of SiO<sub>2</sub> in the mineral's  
14 structure has a considerable impact on the temperature of mercury release. As it can be  
15 seen in Fig. 2D, the peak of mercury desorption from this mineral moved to higher  
16 temperatures than the characteristic peak of HgS (Fig. 2D). This result suggests that the  
17 SiO<sub>2</sub> in myrickite makes the binding of mercury stronger than in pure HgS. This  
18 behavior was not observed when HgS and SiO<sub>2</sub> were mixed from individual species  
19 (Lopez-Anton et al. 2010; Rumayor et al. 2013). Therefore, myrickite becomes an  
20 essential natural standard to be considered in HgTPD analysis.

21 Terlinguaite is a naturally occurring mineral with the formula Hg<sub>2</sub>ClO that is  
22 formed by weathering of other mercury minerals (Hillebrand and Schaller 1907). Its  
23 color is greenish yellow (Fig. 1D). The association of mercury with chlorine and oxygen  
24 in the terlinguaite sample studied was demonstrated by SEM/EDAS (Fig. 5b).  
25 Terlinguaite showed a wide band between 300-1000°C (Fig. 2E). A narrow peak at

1 approximately 40°C due to the impurity of elemental mercury is observed. The wand  
2 band, which could be characteristic of this mineral, does not correspond to the signal of  
3 any of the pure mercury compounds studied so far. The high temperature that it is  
4 necessary to decompose this mineral (close to 1000°C) would explain why some  
5 researchers (Bloom et al. 2002; Staun et al. 2018) have observed that a variety of  
6 samples require temperatures above 900 °C to achieve complete liberation of mercury,  
7 and suggest that is due to an association with refractory silicates. According to  
8 SEM/EDAS (Fig. 5b), a remarkable concentration of Si is present in this mineral  
9 sample, with what the Hg<sub>2</sub>ClO-Si association cannot be ruled out.

10 Corderoite is a mercury sulfide chloride mineral (Hg<sub>3</sub>S<sub>2</sub>Cl<sub>2</sub>) (Fig. 1E) that occurs as  
11 isolated grains or together with cinnabar. Corderoite occurs as a low temperature  
12 supergene mineral (Foord et al. 1974). The analysis of its particles by SEM/EDAS  
13 showed that the sample studied did not contain other mercury species in significant  
14 concentrations (Fig. 6b). However, the thermogram of this mineral made it possible to  
15 identify three mercury species: Hg<sup>0</sup>, HgCl<sub>2</sub> and HgS (Fig. 2F). The presence of three  
16 possible peaks when the desorption profile was deconvoluted suggests that the thermal  
17 decomposition of Hg<sub>3</sub>S<sub>2</sub>Cl<sub>2</sub> could take place during desorption, and this could happen  
18 via reactions 1 and 2 (Lopez-Anton et al. 2010; Rumayor et al. 2013; Cotte et al. 2006).



21 At this point it should be mentioned that analysis by HgTPD would also allow to  
22 follow the effect of temperature on the decomposition of the mercury species.

23 Livingstonite (HgSb<sub>4</sub>S<sub>8</sub>) is a mercury mineral of a gray steel color (Fig. 1F). It  
24 occurs in low-temperature hydrothermal veins mainly associated with cinnabar, stibnite,

1 sulfur and gypsum. Particles containing Hg/Sb/S were identified by SEM/EDAS  
2 analysis (Fig. 7a). Its thermal behavior was similar to that observed for pure HgS, with a  
3 maximum decomposition temperature of approximately 155°C (Table 1, Fig. 2G). The  
4 presence of Sb did not modify the thermal behavior of pure HgS.

5 The identification of mercury species was completed with the inclusion of the  
6 thermal profile of edgarbaileyite, ( $\text{Hg}_6\text{Si}_2\text{O}_7$ ) (Fig. 1G), the first structure reported to  
7 contain both Hg and Si (Fig. 8). It occurs as a secondary mineral and is probably the  
8 result of the reaction of mercury with quartz in conditions that so far have not been  
9 completely understood (Angel et al. 1990). The results of HgTPD (Fig. 2H) showed the  
10 following signals: (i) a narrow peak corresponding to  $\text{Hg}^0$ . As occurred in terlinguaite  
11 and corderoite, it is an impurity that is often found in these types of mercury minerals,  
12 (ii) a short peak at approximately 150°C corresponding to HgS, the most abundant  
13 mercury mineral in nature and probably present as an impurity and (iii) a broad band  
14 between 200-850°C with two main peaks corresponding to HgO (Table 1). As it can  
15 also be observed (Fig. 2A and 2H), the height of each of the HgO peaks depends on the  
16 sample matrix.

17 It must be emphasized that sulfurized mercury minerals like myrickite ( $\text{HgS SiO}_2$ )  
18 or corderoite ( $\text{Hg}_3\text{S}_2\text{Cl}_2$ ) showed different thermograms than those obtained for pure  
19 HgS. Thus, HgTPD may be a useful tool to help understand the possible degradation or  
20 change of color of cinnabar (HgS) in different materials.

21

## 22 **4. Conclusions**

23 Thermal desorption profiles of mercury rare minerals and mercury species in  
24 mineral matrices are presented for the first time. Different profiles were obtained

1 depending on the mineral and the type of mercury association in the mineral. The results  
2 confirm that certain species of mercury are desorbed at the same temperature regardless  
3 of their matrix (livingstonite, coloradoite). However, certain matrices can affect the  
4 desorption temperature of mercury species ( $\text{HgS}$   $\text{SiO}_2$  (myrickite)). This is very  
5 important when comparing mercury desorption temperatures of real samples with those  
6 obtained with mercury standards prepared in the laboratory.

7 The data obtained in the analysis of minerals containing mercury performed in this  
8 work allow the HgTPD technique to be applied to the identification of possible  
9 uncommon sources of mercury pollution in areas such as mining where some of the  
10 minerals studied in this work might be found. Moreover, unlike most commercial  
11 analyzers, the HgTPD device employed in this work may reach temperatures of  $950^\circ\text{C}$ ,  
12 making it possible to identify unknown refractory mercury bearing phases.

13

#### 14 **Acknowledgments**

15 The authors acknowledge the financial assistance received under project GRUPIN14-  
16 031 and thank the Spanish Ministry of Economy and Competitiveness for awarding a  
17 “Ramón y Cajal” postdoctoral contract (RYC-2013-12596) to M.A. López-Antón.

18

#### 19 **References**

- 20 Angel RJ, Gressey G, Criddle A (1990) Edgarebileyite,  $\text{Hg}_6\text{Si}_2\text{O}_7$ : The crystal structure  
21 of the first mercury silicate. *Am Mineral* 75:1192-1196.
- 22 Biester H, Müller G, Schöler HF (2002) Binding and mobility of mercury in soils  
23 contaminated by emissions from chlor-alkali plants. *Sci Total Environ* 284:191-203.
- 24 [https://doi.org/10.1016/S0048-9697\(01\)00885-3](https://doi.org/10.1016/S0048-9697(01)00885-3).

- 1 Biester H, Scholz C (1996) Determination of Mercury Binding Forms in Contaminated  
2 Soils: Mercury Pyrolysis versus Sequential Extractions. *Environ Sci Technol* 31:233-  
3 239. <https://doi.org/10.1021/es960369h>.
- 4 Bloom NS, Preus E, Katon J, Hiltner M (2003) Selective extractions to assess the  
5 biogeochemically relevant fractionation of inorganic mercury in sediments and soils.  
6 *Anal Chim Acta* 479:233-248. [https://doi.org/10.1016/S0003-  
7 2670\(02\)01550-7](https://doi.org/10.1016/S0003-2670(02)01550-7)
- 8 Bloom NS, Vondergeest V, Preus E (2002) Intercomparison of four methods for the  
9 determination of total mercury in recalcitrant solids. Annual Meeting of SETAC  
10 Europe, 347-348, Vienna.
- 11 Cotte M, Susini J, Metrich N, Moscato A, Gratzu C, Bertagnini A, Pagon M (2006)  
12 Blackening of Pompeian cinnabar paintings: X-ray microspectroscopy analysis. *Anal*  
13 *Chem* 78:7484-7492. <https://doi.org/10.1021/ac0612224>.
- 14 Fadda S, Fiori M, Grillo SM. (2005) Chemical variations in tetrahedrite - tennantite  
15 minerals from the Furtei epithermal Au deposit, Sardinia, Italy: Mineral zoning and  
16 ore fluids evolution. *Geochemistry, Mineralogy and Petrology*. Bulgarian Academy  
17 of Sciences. 43:79–84.
- 18 Foord EE, Berendsen P, Storey LO (1974) Corderoite, first natural occurrence of  
19  $\text{Hg}_3\text{S}_2\text{Cl}_2$ , from the Cordero mercury deposit, Humboldt County, Nevada. *Am*  
20 *Mineral* 59:652–655.
- 21 Grammatikopoulos TA, Valeyev O, Roth T (2006) Compositional variation in Hg-  
22 bearing sphalerite from the polymetallic Eskay Creek deposit, British Columbia,  
23 Canada. *Chemie der Erde – Geochemistry* 66:307-314.  
24 <http://doi:10.1016/j.chemer.2005.11.003>.

1 Han Y, Kingston HM, Boylan HM, Rahman GMM, Shah S, Richter RC, Link DD,  
2 Bhandari S (2003) Speciation of mercury in soil and sediment by selective solvent  
3 and acid extraction. *Anal Bioanal Chem* 375:428-436.  
4 <https://doi.org/10.1007/s00216-002-1701-4>.

5 Hillebrand WF, Schaller WT (1907) The Mercury Minerals from Terlingua, Texas:  
6 Kleinite, Terlinguaite, Eglestonite, Montroydite, Calomel, Mercury. *J Am Chem*  
7 *Soc* 29:1180-1194

8 Huggins FE, Yap N, Huffman GP, Senior CL (2003) XAFS characterization of mercury  
9 captured from combustion gases on sorbents at low temperatures. *Fuel Process*  
10 *Technol* 82:167-196. [https://doi.org/10.1016/S0378-3820\(03\)00068-7](https://doi.org/10.1016/S0378-3820(03)00068-7).

11 Issaro N, Abi-Ghanem C, Bermond A (2009) Fractionation studies of mercury in soils  
12 and sediments: A review of the chemical reagents used for mercury extraction.  
13 *Anal Chim Acta* 631:1-12. <https://doi.org/10.1016/j.aca.2008.10.020>.

14 Jiménez-Moreno M, Barre JPG, Perrot V, Bérail S, Rodríguez Martín-Doimeadios RC,  
15 Amouroux D (2016) Sources and fate of mercury pollution in almadén mining  
16 district (Spain): Evidences from mercury isotopic compositions in sediments and  
17 lichens. *Chemosphere* 147:430-438. <https://doi:10.1016/j.chemosphere.2015.12.094>

18 Kim CS, Bloom NS, Rytuba JJ, Brown GE (2003) Mercury Speciation by X-ray  
19 Absorption Fine Structure Spectroscopy and Sequential Chemical Extractions: A  
20 Comparison of Speciation Methods. *Environ Sci Technol* 37:5102-5108.  
21 <https://doi.org/10.1021/es0341485>.

22 Kim CS, Rytuba JJ, Brown GE (2004) EXAFS study of mercury(II) sorption to Fe- and  
23 Al-(hydr)oxides II. Effects of chloride and sulfate. *J Colloid Interf Sci* 270:9-20.  
24 <https://doi.org/10.1016/j.jcis.2003.07.029>.

- 1 Kobal AB, Snoj Tratnik J, Mazej D, Fajon V, Gibičar D, Miklavčič A, Kocman D,  
2 Kotnik J, Sešek Briški A, Osredkar J, Krsnik M, Prezelj M, Knap Č, Križaj B, Liang  
3 L, Horvat M (2017) Exposure to mercury in susceptible population groups living in  
4 the former mercury mining town of idrija, slovenia. *Environ Res* 152:434-445.  
5 <https://doi:10.1016/j.envres.2016.06.037>.
- 6 Kozin LF, Hansen SC, Zakharchenko NF, Gray J (2013) CHAPTER 12 Environmental  
7 Aspects of the Industrial Application of Mercury, in: *Mercury Handbook: Chemistry,*  
8 *Applications and Environmental Impact.* The Royal Society of Chemistry, pp. 209–  
9 227. <https://doi.org/10.1039/9781849735155-00209>.
- 10 Lopez-Anton MA, Yuan Y, Perry R, Maroto-Valer MM (2010) Analysis of mercury  
11 species present during coal combustion by thermal desorption. *Fuel* 89:629-634.  
12 <https://doi.org/10.1016/j.fuel.2009.08.034>.
- 13 Matanzas N, Sierra MJ, Afif E, Díaz TE, Gallego JR, Millán R (2017) Geochemical  
14 study of a mining-metallurgy site polluted with as and hg and the transfer of these  
15 contaminants to *equisetum* sp. *J Geochem Explor* 182:1-9.  
16 <http://doi:10.1016/j.gexplo.2017.08.008>.
- 17 Ozerova NA (1996) Mercury in geological systems, in: *Global and Regional Mercury*  
18 *Cycles: Sources, Fluxes and Mass Balances.* Edited by Willy Baeyens, Ralf  
19 Ebinghaus and Oleg Vasiliev. Published by Kluwer Academic Publishers, The  
20 Netherlands, pp. 463-474. ISBN-13: 978-94-010-7295-3; DOI: 10.1007/978-94-009-  
21 1780-4; e-ISBN-13: 978-94-009-1780-4
- 22 Rallo M, López-Antón MA, Contreras ML, Maroto-Valer MM (2012) Mercury policy  
23 and regulations for coal-fired power plants. *Environ Sci Pollut R* 19:1084-1096.  
24 <https://doi.org/10.1007/s11356-011-0658-2>

1 Raposo C, Windmüller CC, Junior WAD (2003) Mercury speciation in fluorescent  
2 lamps by thermal release analysis. Waste Manage 23:879-886.  
3 [https://doi.org/10.1016/S0956-053X\(03\)00089-8](https://doi.org/10.1016/S0956-053X(03)00089-8).

4 Reis AT, Coelho JP, Rodrigues SM, Rocha R, Davidson CM, Duarte AC, Pereira E  
5 (2012) Development and validation of a simple thermo-desorption technique for  
6 mercury speciation in soils and sediments. Talanta 99:363-638.  
7 <https://doi.org/10.1016/j.talanta.2012.05.065>.

8 Rumayor M, Díaz-Somoano M, López-Antón MA, Martínez-Tarazona MR (2013)  
9 Mercury compounds characterization by thermal desorption. Talanta 114:318-322.  
10 <https://doi.org/10.1016/j.talanta.2013.05.059>.

11 Rumayor M, Lopez-Anton MA, Díaz-Somoano M, Martínez-Tarazona MR (2015a) A  
12 new approach to mercury speciation in solids using a thermal desorption technique.  
13 Fuel 160:525-530. <https://doi.org/10.1016/j.fuel.2015.08.028>.

14 Rumayor M, López-Antón MA, Díaz-Somoano M, Martínez-Tarazona MR (2015b)  
15 Device for identification of mercury species in solids. Consejo Superior de  
16 Investigaciones Científicas (CSIC). Patent ES1641.1031 Application number:  
17 P201530310.

18 Rumayor M, López-Antón MA, Díaz-Somoano M, Maroto-Valer MM, Richard J-H,  
19 Biester H, Martínez-Tarazona MR (2016) A comparison of devices using thermal  
20 desorption for mercury speciation in solids. Talanta 150:272-277.  
21 <https://doi.org/10.1016/j.talanta.2015.12.058>.

22 Staun C, Vaughan J, Lopez-Anton MA, Rumayor M, Martínez-Tarazona M.R (2018)  
23 Geochemical speciation of mercury in bauxite. Appl Geochem 93:30-35.  
24 <https://doi.org/10.1016/j.apgeochem.2018.03.007>.

25 WHO (2017) World Health Organization. [http://www.who.int/news-room/fact-](http://www.who.int/news-room/fact-sheets/detail/mercury-and-health)  
26 [sheets/detail/mercury-and-health](http://www.who.int/news-room/fact-sheets/detail/mercury-and-health)

1 Yin R, Zhang W, Sun G, Feng Z, Hurley JP, Yang L, Shang L, Feng X (2017) Mercury  
2 risk in poultry in the wanshan mercury mine, china. Environ Pollut 230:810-816.  
3 <http://doi:10.1016/j.envpol.2017.07.027>.

4

5

1 **Table 1** Characteristic maximum temperature of desorption corresponding to pure  
2 mercury compounds.

<b>Mercury compound</b>	<b>High peak T (°C)</b>
Hg <sup>0</sup>	46±10
HgCl <sub>2</sub>	116±9
HgS black	160±12
HgO	280±10; 480±10

3

4

1  
2  
3  
4  
5  
6  
7  
8  
9  
10  
11  
12  
13  
14  
15  
16  
17  
18  
19  
20  
21  
22  
23  
24  
25  
26  
27

**Figure captions**

**Fig. 1** Photographs of mineral samples containing mercury.

**Fig. 2** Thermal profiles of A) mercury pure compounds ( $\text{Hg}^0$ ,  $\text{HgCl}_2$ ,  $\text{HgS}$ ,  $\text{HgO}$ ), B) sphalerite, C) coloradoite, D) myrickite, E) terlinguaite, F) corderoite, G) livingstonite and H) edgarbaileyite).

**Fig. 3** EDX analysis and SEM images of sphalerite.

**Fig. 4** EDX analysis and SEM images of coloradoite.

**Fig. 5** EDX analysis and SEM images of myrickite and terlinguaite.

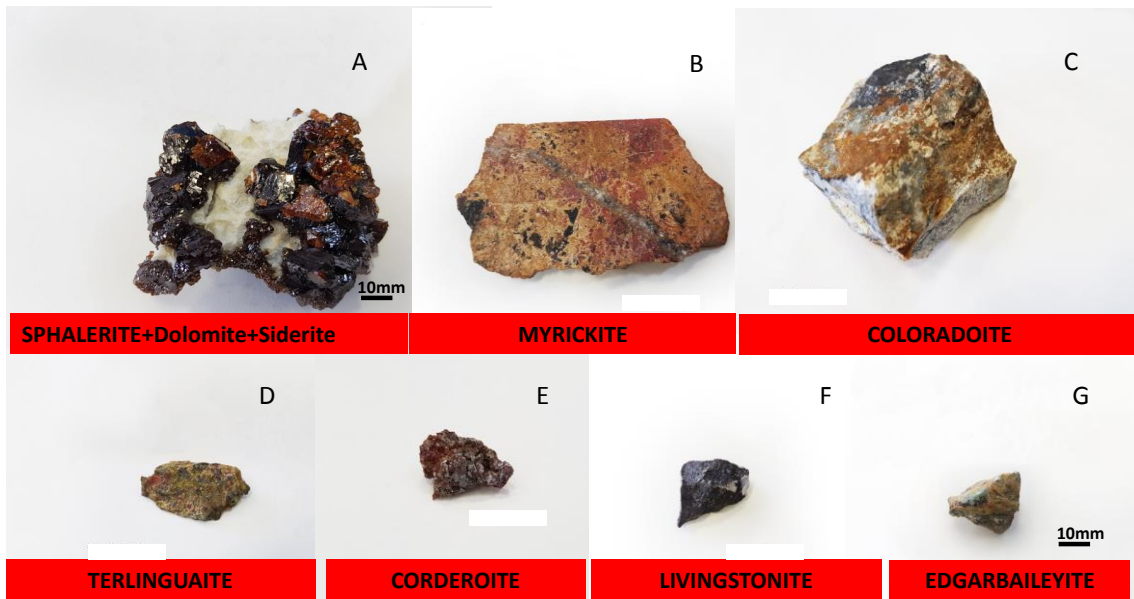
**Fig. 6** EDX analysis and SEM images of corderoite.

**Fig. 7** EDX analysis and SEM images of livingstonite.

**Fig. 8** EDX analysis and SEM images of edgarbaileyite.

1

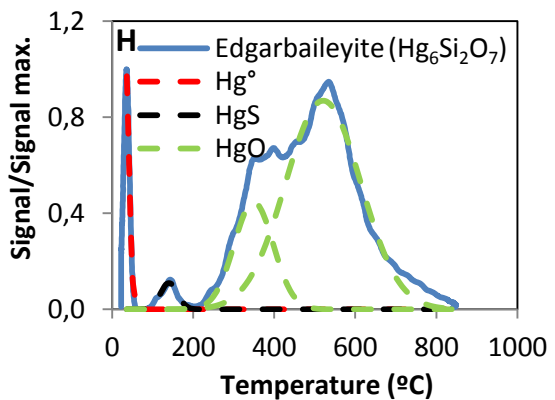
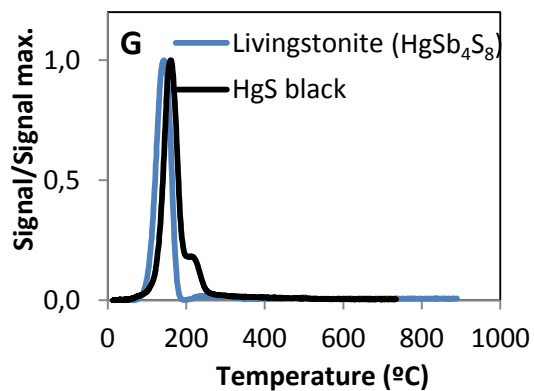
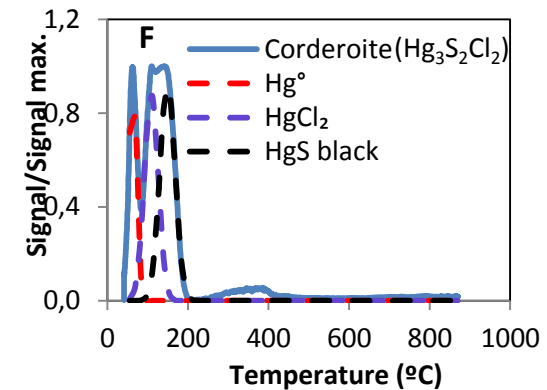
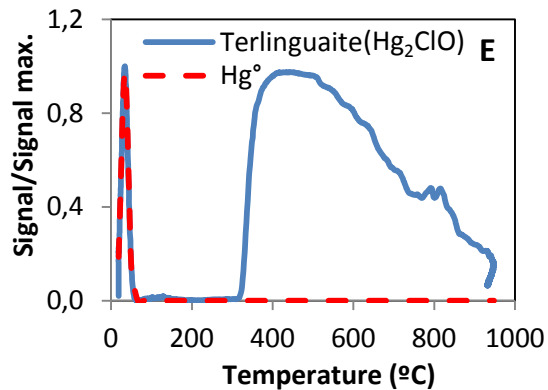
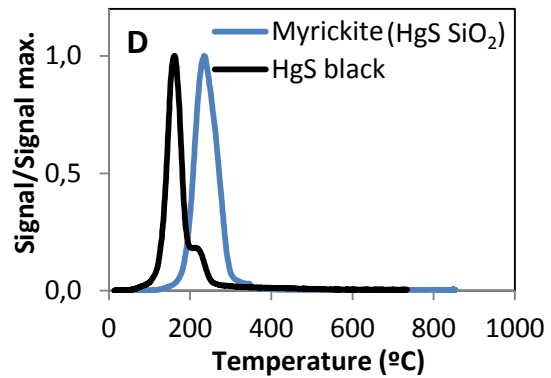
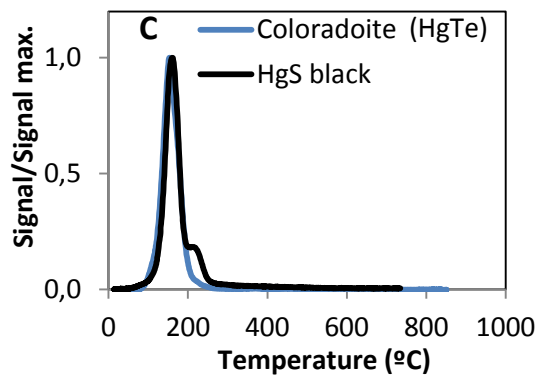
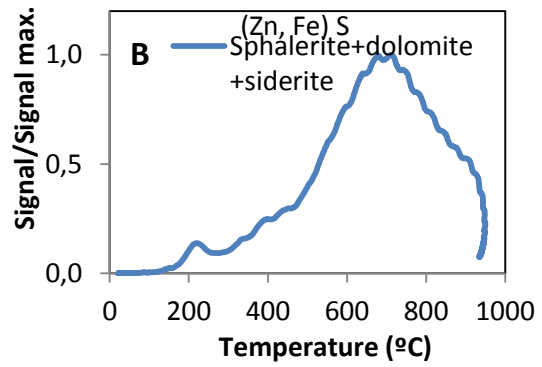
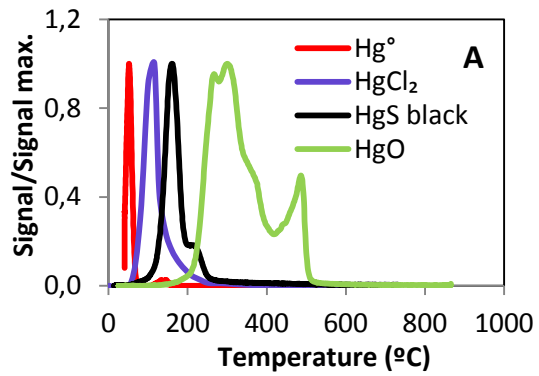
2



3

4 Fig. 1

5



1

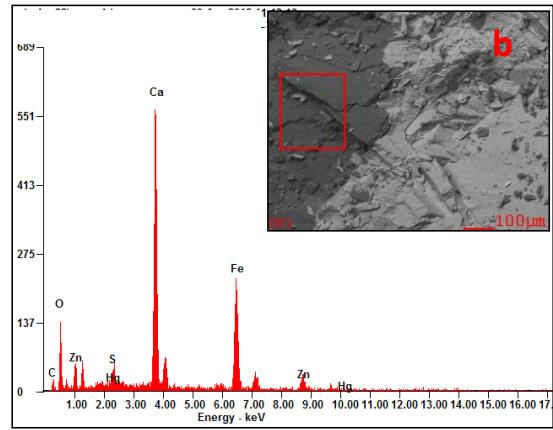
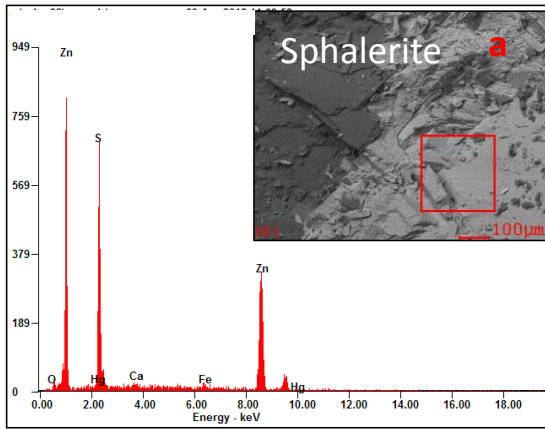
2

3

4

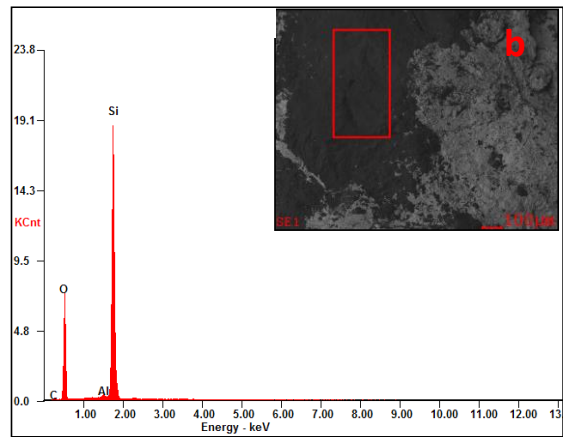
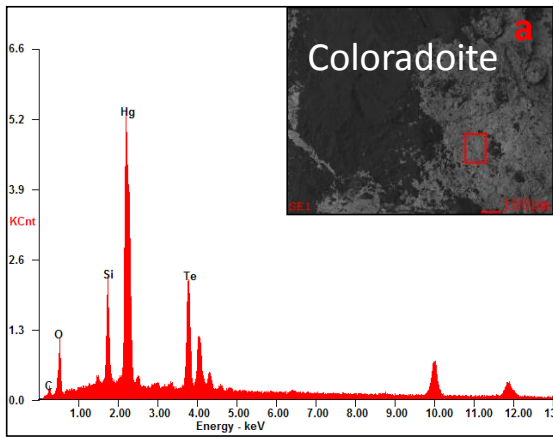
5 Fig. 2

1



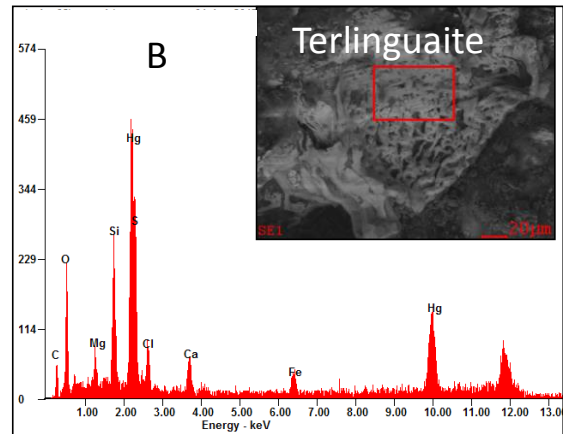
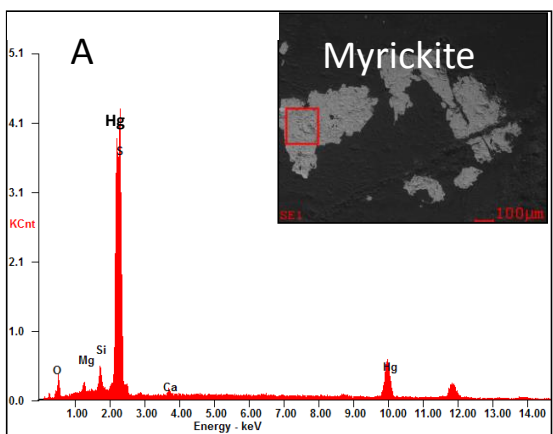
2

3 Fig. 3



4

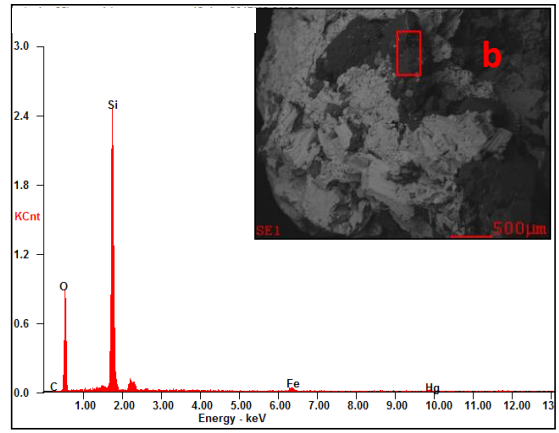
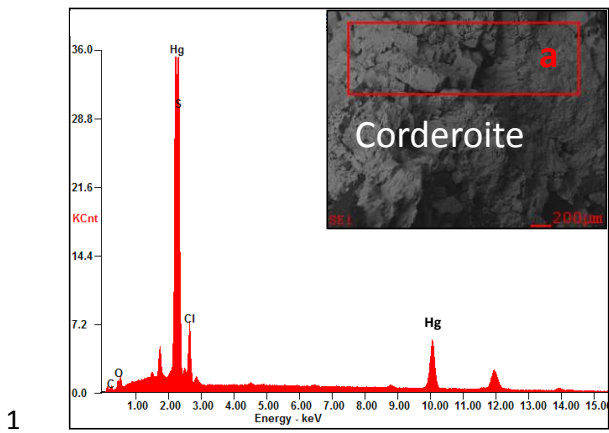
5 Fig. 4



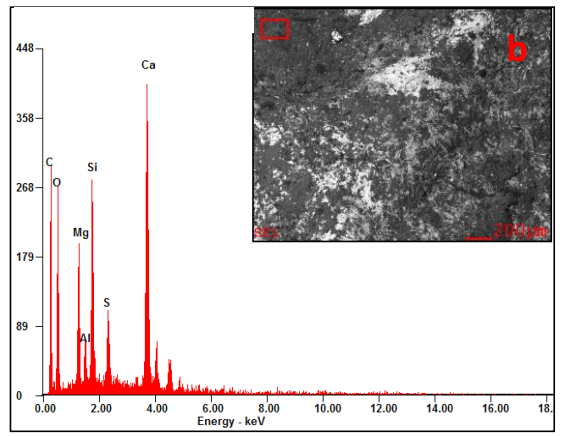
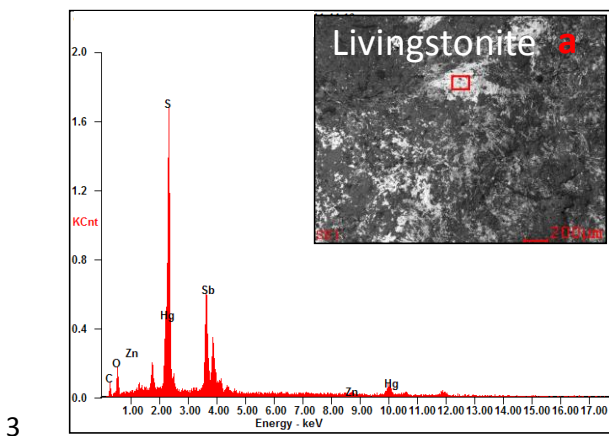
6

7

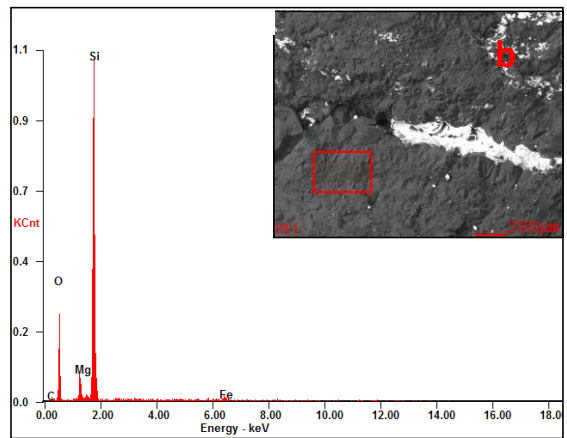
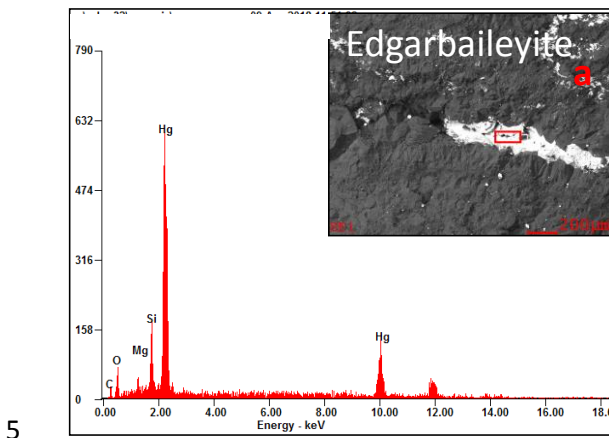
8 Fig. 5



2 Fig. 6



4 Fig. 7



6 Fig. 8

7